AUBE '01

12TH INTERNATIONAL CONFERENCE ON AUTOMATIC FIRE DETECTION

March 25 - 28, 2001
National Institute Of Standards and Technology
Gaithersburg, Maryland U.S.A.

PROCEEDINGS

Editors: Kellie Beall, William Grosshandler and Heinz Luck

NIST
National Institute of Standards and Technology
Technology Administration, U.S. Department of Commerce

O. Keski-Rahkonen
VTT Building and Transport, P.O. Box 1803, FIN-02044 VTT, Finland
Olavi.Keski-Rahkonen@vtt.fi

Revisiting modelling of fluid penetration into smoke detectors for low speed ceiling jets

1. Introduction

A smoke detector is in principle a container, which has partially permeable walls separating the gas volume in the detector from the volume around it. Walls delay fire detection as compared to a fully open detector. Heskestad [1] drafted a theory using dimensional analysis arguments for the time lag Δt of a products-of-combustion fire detector

$$\Delta t = \gamma \, l / \bar{v} \qquad (1)$$

where $\bar{v}$ is the mean convective flow velocity around the point detector, l the characteristic length scale, and γ a non-dimensional coefficient characteristic for the geometry. According to [1] Eq. (1) is valid presuming 'viscosity effects are not considered important'.

Brozovsky [2] observed the simple relationship of Eq. (1) did not hold for low ceiling jet velocities. In Fig. 1 his observations (dots) are plotted as a function of velocity $\bar{v}$. Thin solid lines represent exponential fits by Brozovsky [2] on his limited set of data. Further data manipulation showed, an equation of the form

$$\Delta t = \gamma l /(\bar{v} - \bar{v}_0) \qquad (1')$$

is also a plausible fit on the data. The numerical values of the parameters were: γl = 0.8 m and $\bar{v}_0$ = 0.075 m/s, which Brozovsky called a critical velocity. Fitting Heskestad's correlations on these data according to Eq. (1) would yield curves similar to # 1 and # 2 in Fig. 1. These predictions are in contrast with experiments. No value of γl would fit experimental data.

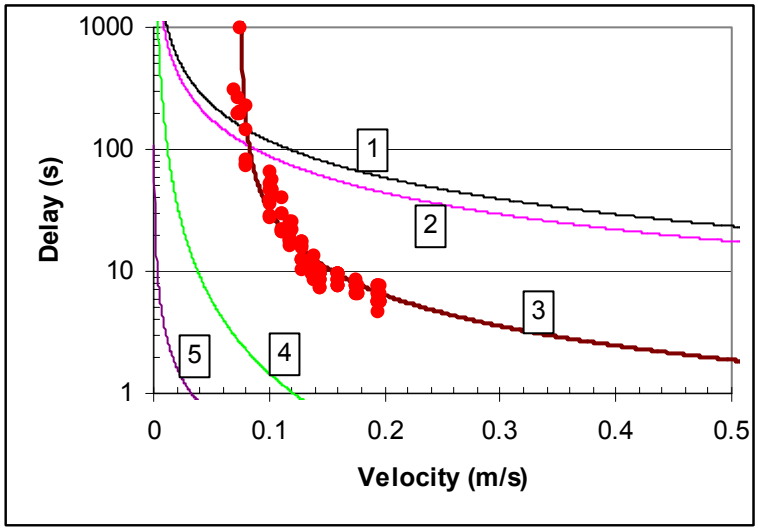

Fig. 1. Entry lag time dependence on flow velocity past a detector. Dots (experimental data). (1) and (2): The delay time according to Eq. (1) as explained in text. (3): Fit according to Eq. (1'), $\bar{v}_0$ *= 0.075 m/s). (4) and (5) Calculated models explained in text.*

2. Flow and pressure fields around solid bodies

2.1 Principles of calculation

There is a wealth of literature on flow around solid objects in a flow field using different techniques at different level of approximation [6 - 10]. No general analytical solutions are available for all flow velocities. Furthermore, in the whole body of this literature only some references were given on works, where the body is partially transparent [7 - 8]. For these reasons here general techniques of flow modelling are attempted in the regions, where analytical solutions are available. Flow through the detector is treated as perturbation. To grasp the salient physics of the flow we first calculate the pressure field around a totally solid body for a constant velocity, and use that information to calculate flow through the mesh in and out of the fire detector. The validity of perturbation approach is not granted. Failure of it demonstrated by related

drag problem. Despite that, analytical approaches are so simple, it was decided to try them first. For calculating the flow around the detector Reynolds numbers are typically 100 ... 1000. For flow through the mesh Reynolds numbers are in the range 0.1 ... 10. Therefore, the calculation can be made in two stages, and requires different approximations in both ranges.

A smoke detector can be modelled as a solid object in a flow field, which is partially permeable. For modelling we set the center of the detector in origin, and arrange a flow along the negative x-axis with a velocity v_∞ far from the origin towards positive x. The point on the detector, where negative x-axis penetrates the outer surface is a stagnation point. On the opposite lee side, there is a point, where the dynamic pressure is the lowest. For the smoke flow through the detector the insect mesh provides the biggest flow resistance. Without quantitative calculations, only through visual inspection of some detector constructions all other channels of the flow have much bigger cross sections, and relative to the mesh penetration pressure drop can be considered only as small.

Therefore we concentrate here only on the ultimately simplified geometrical model of the detector: (i) a cylindrical or hemispherical outer mesh, (ii) small channels through the mesh into (iii) the interior of the detector of total volume V. Due to additional light scattering barriers and flow channelling guides inside the detector the volume V is considered a well stirred reactor, which communicates with the space outside the insect mesh through the holes on it. The other alternative in the inner space is to use laminar plug flow, and calculate time of smoke front moving from the mesh the center point. For a smoke detector two geometrical, highly idealized models are used: (a) a two dimensional, infinitely long circular cylinder neglecting the presence of the ceiling, and (b) a three dimensional hemisphere setting the frictionless ceiling in the equatorial plane. First, potential flow is applied to both problems to account for the disturbance the detector causes on the free flow field.

For calculation we set the coordinate system as shown in Fig. 2. The origin O is set to the center of the detector in the plane of the ceiling. Perpendicular to the plane of the

ceiling and along the center axis of the detector points the z-axis downwards. The detector screen is cylindrical or spherical showing as circle in the x-y-plane of Fig. 2. The screen is partially permeable for the flow, and idealized to a surface of zero thickness. The ceiling jet is assumed to be a free constant velocity flow approaching the detector parallel to the x-axis far left. The detector screen divides the space into two regions: (1) inside, and (2) outside. For modelling flow equations are written for both regions, and boundary conditions along the surface presenting the screen bound the regions together.

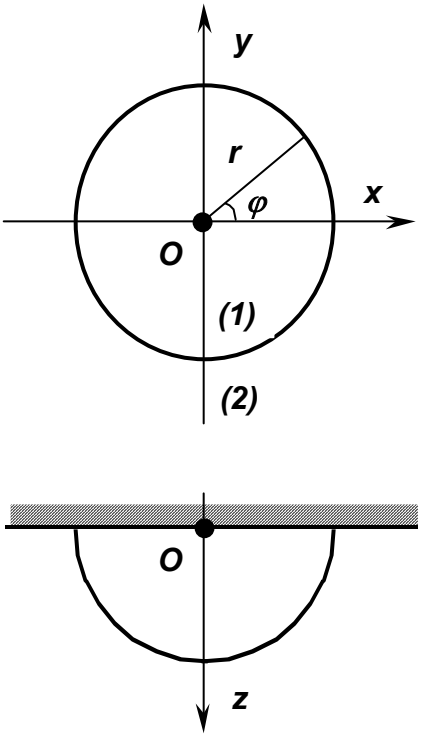

F*igure 2. Coordinate system used for detector modelling.*

2.2 Inviscid potential flow

Experimenting with different combinations of boundary conditions between the inside and outside regions showed, that no extra effects were obtainable. Therefore, potential flow a free stream of velocity v_∞ is superposed with a two (cylinder) or three (sphere)

dimensional doublet [8]. For solid bodies the radial velocity component v_r disappears on the surface. For a permeable body the first order perturbation theory is attempted, which would as mismatch yield to radial velocity distribution

$$v_r = \varepsilon \cos\varphi \tag{2}$$

where the numerical value of ε is determined using experimental pressure distribution around the body slightly simplified [7]. For laminar flow from the stagnation point to the separation angle the φ_k the velocity obeys Eq. (2), after which it has a constant value reached at separation point. The experimental pressure amplitude for laminar flow is

$$p_s - p_k = q\rho v_\infty^2 \tag{3}$$

where $q \approx 1$ for a cylinder and 0.75 for a sphere. For turbulent flow the pattern is similar, but numerical values of q differ slightly. The flow was not yet turbulent around the detector, and thus this combination is not discussed further.

2.3 Laminar viscous flow

A creeping laminar flow past a cylinder results in a logarithmic singularity (Stokes paradox) but past a sphere (Stokes's first problem) the pressure distribution is

symmetric, given on the surface by [10]

$$p = p_\infty - \frac{3\mu v_\infty}{2a}\cos\varphi \tag{4}$$

By coupling to that field an additional radial flow velocity component into the sphere in the form of Eq. (2), it can be shown to be of the higher order in perturbation expansion than the second therm in the pressure distribution of Eq. (4). Therefore, two-stage

calculation is plausible. The flow inside the sphere satisfying Navier-Stokes equations to the same degree of approximation as for the outer flow takes place at constant velocity parallel to the flow far from the detector. Oseen has extended the calculation of Stokes as a power series of Reynolds number [11]. The second term of pressure averages to zero over the sphere. Therefore, it is not taken here as a separate case.

3 Flow through small openings

Calculating the smoke density inside the detector for a flow, where particles do not separate from the fluid, the time constant τ_w of well stirred volume V is given asymptotically by

$$\tau_w = V / \dot{V} \tag{5}$$

where $\dot{V}$ volume flow in the detector. For a plug flow a similar time constant τ_p is obtained by dividing the radius of the detector by the average velocity inside the detector. Both concepts are used here.

When the flow is laminar inviscid through the mesh volume flow is proportional to the square root of pressure difference [7].

For viscid creeping fluid the flow through the holes takes place in a layer attached onto the surface of the mesh. For an order of magnitude estimate we look fully developed viscous flow, which can be solved accurately in a closed form for rectangular channels (Poiseulle flow) [7] or for circular tubes (Hagen-Poiseulle flow) [6 - 7]. Taking the circular variation volume flow $\dot{V}$ through a hole of radius a is given by

$$\dot{V} = -\frac{\pi}{8}\frac{r_0^4}{\eta}\frac{dp}{ds} \tag{6}$$

where η is the dynamic viscosity of air, dp/ds the pressure drop along the channel, and the radius of the circular hole r_0 . In Table 1 calculation forms are given for the lag time τ_w (s) for different reasonable combinations of ambient and grid flow conditions. The formulas are preceeded by numerical factors c_i. Radius of the detector is a, ratio of

combined hole areas to total grid surface area κ, and effective length of pressure drop through mesh δ. In Fig. 1 these time lags are plotted as a function of velocity v_∞ for all calculated cases using rough estimations of the numerical coefficients c_i in those cases they were not direct results from the derivation of the formulas. This is plausible for an order of magnitude calculations.

Curve # 2 is viscid-viscid combination, and curve # 1 plug flow model for the same case. Curve # 5 is laminar-laminar combination with a very big difference between theory and observations. Curve # 3 presents laminar ambient causing viscid grid flow, which is still rather far from measured data.

Table 1. Lag time τ_w (s) calculation formulas.

	Ambient laminar inviscid	Ambient creeping viscid
Grid laminar inviscid	$c_1 \frac{a}{\kappa v_\infty}$	NA
Grid creeping viscid	$c_2 \frac{\nu a \delta}{\kappa r_0^2 v_\infty^2}$	$c_3 \frac{a^2 \delta}{\kappa r_0^2 v_\infty}$

4. Conclusions

Order of magnitude calculation formulas were derived for the lag time of fire detectors using two different scales of flow: (i) ceiling jet flow around the fire detector, and (ii) flow through the mesh. At different jet velocities different flow approximations apply. The experimental data do not support any of the proposed theoretical models since both the magnitudes of calculated lag times differ considerably from the observations, and asymptotically the theoretical curves do not have a pole at a finite velocity. As for the flow through the mesh, viscosity effects cannot be neglected.

The reason for the negative result is not known for sure. Some guesses could be made to guide further research. Perturbation approach may not be valid, because the distribution might be finite even for a very small flow through the detector. There is an analogy with the drag problem of a sphere [10]. The flow through the grid is never fully developed. This was not taken into account, because of difficulty of modelling.

No apparent experimental errors were found in [2]. Therefore, the behaviour described by Eq. (1') seems to indicate the flow might have a 'non-newtonian' character plugging the flow at velocities lower than $\bar{v}_0$. Qualitatively, such a flow occurs, if the fluid, which here is an aerosol, behaves collectively like a non-newtonian continuum fluid of Bingham plastic [3]. The analytical theories of such fluids would in principle allow calculation of the flow in and out of the detector [4, 5]. However, there seemed not be available experimental data of rheological properties of smoke. The tacit assumption has always been, smoke behaves like air, an almost perfect newtonian fluid. 'Non-newtonian' behaviour might also be caused by electric rather than fluid phenomena. Most of the smoke particles are charged. They might stick on the grid at low velocities. However, without further detailed experimental observations, if not yet readily available, these questions cannot be settled.

Acknowledgements

This study has been partially financed by the Finnish Centre for Radiation and Nuclear Safety, the Ministry of Trade and Industry, Fortum Engineering Ltd, Teollisuuden Voima Oy, and the Finnish Fire Research Board. I am indebted to E.L. Brozovsky for sending me the original experimental data.

References

[1] Heskestad, G. Generalized Characterization of Smoke Entry and Responce for Products-of-Combustion Detectors, Fire Detection of Life Safety, Proceedings of a Symposium, March 31 and April 1, 1975, National Academy of Sciences, Washington , D.C., (1977), p. 93 - 127.

[2] Brozovsky, E.L. A Preliminary Approach to Siting Smoke Detectors Based on Design Fire Size and Detector Aerosol Entry Lag Time, Master's Thesis, Worcester Polytechnic Institute, Worcester, MA, 1991, 96 p.

[3] Irvine, T.F., Jr., & Capobianchi, M., 1998. Non-Newtonian Flows, in R.W. Johnson (Ed.) The Handbook of Fluid Dynamics, CRC Press, Boca Raton, Chapter 22.

[4] Kawase, Y. & Moo-Young, M., 1992. Flow and Heat Transfer in Turbulent Slurries, International Communications in Heat and Mass Transfer 19, 485 - 498.

Bukowski, R.W. & Mulholland, G.W. 1978. Smoke Detector Design and Smoke Properties, NBS Technical Note 973, National Bureau of Standards, Washington, D.C., 51 p.

[5] Patel, N. & Ingham, D.B., 1994. Flow and Heat Transfer in Turbulent Slurries, International Communications in Heat and Mass Transfer 21, 75 - 84.

[6] Frank, P. & von Mises, R. 1943. Die Differential- und Integralgleichungen der Mechanik und Physik, Mary S. Rosenberg, New York, 2. Auglage, 1106 p.

[7] Truckenbrodt, E., 1980. Fluidmechanik, Springer, Berlin, Band 1, 371 p., Band 2, 426 p.

[8] Katz, J. & Potkin, A. 1991. Low Speed Aerodynamics, McGraw-Hill, New York, 632 p.

[9] Kirchhoff, R. H. 1998. Inviscid Incompressible Flow - Potential Flow, in R.W. Johnson (Ed.) The Handbook of Fluid Dynamics, CRC Press, Boca Raton, Chapter 7.

[10] Gursul, I. 1998. Incompressible Laminar Viscous Flows, in R.W. Johnson (Ed.) The Handbook of Fluid Dynamics, CRC Press, Boca Raton, Chapter 9.

[11] Clift, R., Grace, J.R. & Weber, M.E. 1978. Bubbles, Drops, and Particles, Academic, New York, 380 p.